# Abnormal functional connectivity between motor cortex and pedunculopontine nucleus following chronic dopamine depletion

**Miguel Valencia,[1] Mario Chavez,[2] Julio Artieda,[1] J. Paul Bolam,[3] and Juan Mena-Segovia[3]**

[1]*Neurophysiology Laboratory, Neuroscience Area, CIMA, Universidad de Navarra, Pamplona, Spain;* [2]*L'Institut du Cerveau et de la Moelle Épinière, Hôpital de La Pitié-Salpêtrière, Paris, France; and* [3]*MRC Anatomical Neuropharmacology Unit, Department of Pharmacology, University of Oxford, Oxford, United Kingdom*

**Valencia M, Chavez M, Artieda J, Bolam JP, Mena-Segovia J.** Abnormal functional connectivity between motor cortex and pedunculopontine nucleus following chronic dopamine depletion. *J Neurophysiol* 111: 434–440, 2014. First published October 30, 2013; doi:10.1152/jn.00555.2013.—The activity of the basal ganglia is altered in Parkinson's disease (PD) as a consequence of the degeneration of dopamine neurons in the substantia nigra pars compacta. This results in aberrant discharge patterns and expression of exaggerated oscillatory activity across the basal ganglia circuit. Altered activity has also been reported in some of the targets of the basal ganglia, including the pedunculopontine nucleus (PPN), possibly due to its close interconnectivity with most regions of the basal ganglia. However, the nature of the involvement of the PPN in the pathophysiology of PD has not been fully elucidated. Here, we recorded local field potentials in the motor cortex and the PPN in the 6-hydroxydopamine (6-OHDA)-lesioned rat model of PD under urethane anesthesia. By means of linear and nonlinear statistics, we analyzed the synchrony between the motor cortex and the PPN and the delay in the interaction between these two structures. We observed the presence of coherent activity between the cortex and the PPN in low (5–15 Hz)- and high (25–35 Hz)-frequency bands during episodes of cortical activation. In each case, the cortex led the PPN. Dopamine depletion strengthened the interaction of the low-frequency activities by increasing the coherence specifically in the theta and alpha ranges and reduced the delay of the interaction in the gamma band. Our data show that cortical inputs play a determinant role in leading the coherent activity with the PPN and support the involvement of the PPN in the pathophysiology of PD.

pedunculopontine; alpha oscillations; gamma oscillations; parkinsonian; nonlinear interactions

THE PEDUNCULOPONTINE NUCLEUS (PPN) is located in the brain stem and is closely connected to the basal ganglia (Mena-Segovia et al. 2004). It receives dense projections arising mainly in the substantia nigra pars reticulata (SNR; inhibitory) and the subthalamic nucleus (STN; excitatory; for a review, see Martinez-Gonzalez et al. 2011). The close interconnections with the basal ganglia and the reported hyperactivity of the SNR and STN in Parkinson's disease (PD) or its animal models suggest that the PPN is involved in some aspects of the disease (Pahapill and Lozano 2000). For example, cholinergic neurons of the PPN of PD patients have been shown to be reduced in numbers following immunohistochemical labeling (Hirsch et al. 1987), although not changed in some animal models of PD (Heise et al. 2005). Furthermore, deep brain stimulation (DBS) of the PPN is beneficial to relieve some of the symptoms associated with PD (Kringelbach et al. 2007; Moro et al. 2010), in particular those relating to deficits in posture and gait (Caliandro et al. 2011; Thevathasan et al. 2012a,b).

Neurons of the PPN, including cholinergic, GABAergic, and glutamatergic (Mena-Segovia et al. 2009; Wang and Morales 2009), are functionally heterogeneous, and most of them possess variable degrees of coupling to oscillatory activity (Mena-Segovia et al. 2008; Ros et al. 2010). For example, cholinergic neurons can be driven to fire tonically at gamma frequencies when recorded in vitro (Kezunovic et al. 2011) and discharge during specific phases of the cortical oscillations when recorded in vivo (Mena-Segovia et al. 2008). These cholinergic projections thus have the potential to generate distinct effects on a range of oscillatory frequencies, depending on the target (Leszkowicz et al. 2007; Lorincz et al. 2008; Mena-Segovia et al. 2008; Steriade et al. 1991). Furthermore, impairment in the activity of PPN neurons, as a consequence of a pathological process, may result in changes in the oscillatory activity in those structures regulated by PPN afferents and ultimately the cortex. Although the changes in the firing rate of PPN neurons in animal models of PD are inconclusive (Aravamuthan et al. 2008; Breit et al. 2001), an increase in the coherent activity between cortex and PPN during the slow oscillations ($\sim$1 Hz) during urethane anesthesia has been shown (Aravamuthan et al. 2008). In PD, the most prominent motor impairments have been associated with changes in the oscillatory activity across the basal ganglia, particularly in the ranges of alpha (high-voltage spindles; Dejean et al. 2008, 2012) and beta/gamma (Avila et al. 2010; Brown 2006; Lopez-Azcarate et al. 2010; Trottenberg et al. 2006). In addition, recent reports in PD patients who have electrodes implanted in the PPN for DBS show the presence of alpha activity during rest and gait (Androulidakis et al. 2008; Thevathasan et al. 2012b).

Given the oscillatory nature of the output of the PPN, it becomes critical to identify its involvement in the pathophysiology of aberrant oscillatory activity in PD or its animal models. Here, we used the 6-hydroxydopamine (6-OHDA) model of nigrostriatal degeneration to induce parkinsonism in rats and simultaneously recorded the activity of the PPN and the motor cortex (MCx) during periods of cortical activation under anesthesia. We analyzed the data using nonlinear estimators of connectivity and determined the interactions between the PPN and cortex across all frequency bands (1–70 Hz).

## MATERIALS AND METHODS

*Ethics statement.* All experiments were performed in accordance with the Animals (Scientific Procedures) Act 1986 (United Kingdom) under the authority of Project License 30-2639 approved by the Home Office and the local ethical committee of the University of Oxford and the Society for Neuroscience policy on the use of animals in neuroscience.

*6-OHDA lesions.* Unilateral 6-OHDA lesions were performed as described previously (Magill et al. 2001; Mallet et al. 2008; Martinez-Gonzalez et al. 2013). Before surgery, and 25 min before the 6-OHDA injection, Sprague-Dawley rats (250–350 g) received an injection of desipramine (25 mg/kg ip; Sigma, Poole, United Kingdom) to minimize the damage to noradrenergic neurons by blocking the uptake of 6-OHDA. Following stereotaxic placement of a microsyringe in a region adjacent to the medial forebrain bundle (anteroposterior: −4.5; mediolateral: +1.3; dorsoventral: −7.9 mm; bregma: 0; Paxinos and Watson 1986), 3 $\mu$l of a solution of 6-OHDA (Sigma; 4 mg/ml final concentration, 0.9% wt/vol NaCl solution containing 0.02% wt/vol ascorbic acid) were injected over 5 min, allowing a further 5-min period for the drug diffusion. A similar dosage regime has been estimated to produce ~50% loss of tyrosine hydroxylase-positive neurons (Healy-Stoffel et al. 2013). Two to three weeks after the lesion, rats were behaviorally assessed to determine the extent of the dopamine lesion by injecting apomorphine (0.05 mg/kg sc; Sigma; dissolved in 0.9% wt/vol NaCl solution containing 0.02% wt/vol ascorbic acid) and counting the net number of contralateral rotations. A lesion was considered successful when rats made >80 rotations over a 20-min period. Rats with successful lesions were then used for electrophysiological recordings 4–9 wk later (mean: 4.88 wk). Control rats did not receive any treatment (naïve).

*Electrophysiological recordings.* We assessed the electrophysiological activity of the PPN and the cerebral cortex in anesthetized rats (control, $n = 15$; 6-OHDA, $n = 9$) as described previously (Mena-Segovia et al. 2008). Anesthesia was induced with 4% vol/vol isoflurane (IsoFlo; Schering-Plough, Welwyn Garden City, United Kingdom) in $O_2$ and maintained with urethane (1.3 g/kg ip; ethyl carbamate; Sigma) and supplemental doses of ketamine (30 mg/kg ip; Ketaset; Willows Francis, Crawley, United Kingdom) and xylazine (3 mg/kg ip; Rompun; Bayer). The electrocorticogram (ECoG; see below) and reflexes were monitored to ensure the animals' well-being. Body temperature was maintained at 37°C by a feedback temperature controller.

The ECoG was recorded via a 1-mm-diameter steel screw juxtaposed to the dura mater above the frontal cortex (3.0 mm anterior and 2.5 mm lateral to bregma; Paxinos and Watson 1986), which corresponds to the somatic sensorimotor cortex (Donoghue and Wise 1982). The raw ECoG signal was band-pass filtered (0.3–1,500 Hz, −3-dB limits) and amplified (2,000×; DPA-2FS filter/amplifier; Scientifica, Harpenden, United Kingdom) before acquisition. Extracellular recordings in the PPN were made using 15- to 25-M$\Omega$ glass electrodes (tip diameter: ~1.5 $\mu$m) filled with saline solution (0.5 M NaCl) and Neurobiotin (1.5% wt/vol; Vector Laboratories, Peterborough, United Kingdom). Glass electrode signals were amplified (10×) through the active bridge circuitry of an Axoprobe-1A amplifier (Molecular Devices, Sunnyvale, CA), alternating current-coupled, and amplified a further 100× (NL106 AC-DC Amplifier; Digitimer, Welwyn Garden City, United Kingdom) before being band-pass filtered between 0.3 and 5 kHz (NL125; Digitimer). All biopotentials were digitized online using a Power1401 analog-to-digital converter (Cambridge Electronic Design, Cambridge, United Kingdom) and a personal computer running Spike2. ECoG and local field potential (LFP) signals arising in the cortex and PPN, respectively, were then downsampled to a sampling frequency of 1,000 Hz by using the "resample.m" MATLAB (MathWorks, Natick, MA) function. Recording locations were verified using histology after perfusion.

Activity was recorded during episodes of spontaneous or sensory-evoked "global activation," which contain patterns of activity that are more analogous to those observed during the awake state (Steriade 2000). Sensory stimulation and subsequent global activation were elicited by a standard calibrated pinch of the hindpaw delivering a standard pressure of 183 g/mm$^2$ (15 s). The animals did not respond overtly to the pinch. Following the initial effect of the pinch (obliteration of the cortical slow oscillations that are typical of the urethane anesthesia), fast-frequency, low-amplitude activity was observed in the ECoG for variable periods of time, which then returned gradually to slow oscillations. Samples of 60-s segments of continuous recordings from different recording locations across the PPN (control, $n = 31$; 6-OHDA, $n = 28$) were selected offline for further analysis. We allowed ≥1 min separation between the pinch and the selected segment.

*Histological verification.* Following the electrophysiological recordings with glass microelectrodes, the locations of some neurons were verified (Mena-Segovia et al. 2008; Pinault 1996). Briefly, a microiontophoretic current was applied (1- to 10-nA positive current, 200-ms duration, 50% duty cycle) while the electrode was in juxtaposition to the recorded neuron. The modulation of the neuronal firing was maintained for ≥2 min to obtain reliable labeling of the soma. At the end of the experiment, the animals were given a lethal dose of ketamine (150 mg/kg) and intracardially perfused with 0.05 M PBS, pH 7.4, followed by 300 ml of 4% wt/vol paraformaldehyde and 0.1% wt/vol glutaraldehyde in phosphate buffer (0.1 M, pH 7.4). Brains were stored in PBS at 4°C until sectioning. Neurobiotin-labeled neurons were revealed by incubation with Cy3-conjugated streptavidin (1:1,000; Jackson ImmunoResearch Laboratories) as reported before (Mena-Segovia et al. 2008; Ros et al. 2010).

*Spectral analysis.* Welch periodograms (window length: 2 s, overlap: 90%, Hanning window, resolution of ~1 Hz per bin) were used to compute the power spectral density of the ECoG and PPN LFPs.

*Coherence.* Functional relationships between the MCx and the PPN were estimated by means of coherence (Coh). The coherence between two signals is a measure of their linear relationship at a specific frequency (Halliday et al. 1995). It is defined as the normalized cross-spectrum according to:

$$\mathrm{Coh}_{x,y}(f) = \frac{S_{xy}(f)}{\sqrt{S_x(f) \cdot S_y(f)}}$$

where $x(t)$ and $y(t)$ are two random, zero-mean processes and $S_x(f)$, $S_y(f)$, and $S_{xy}(f)$ are the values of their auto- and cross-spectra at a given frequency $(f)$. Coherence provides a normalized measure of the linear correlation between signals in the frequency domain; it ranges from 0 to 1, with 1 for perfect linear association and 0 indicating a complete absence of it. Again, Welch periodograms (window length: 2 s, overlap: 90%, Hanning window, resolution of ~1 Hz per bin) were used to compute the auto- and cross-spectral densities.

*Nonlinear correlation coefficient.* To look further into the degree of statistical association and the time delay between the two brain signals, the nonlinear correlation coefficient ($h^2$) was calculated (Lopes da Silva et al. 1989). Basically, this method quantifies the dependency of a signal $y(t)$ on a signal $x(t)$. To do so, a piecewise linear regression curve is used to predict the signal $y(t)$ given the values of $x(t)$. A practical implementation of this index is obtained by splitting, in a scatterplot, the values of $x(t)$ in $L$ bins (see below). For each bin, the average of the corresponding $y(t)$ values is calculated, the $q_k$ points. The $x$-value of the midpoint of each bin is called $p_k$. Then, the nonlinear regression curve is obtained by connecting the points $(p_k,q_k)$ by segments of straight lines. The estimator of the nonlinear correlation index is computed as follows:

$$h^2(x \rightarrow y) = \frac{\sum_{i=1}^{N}(y_i - \langle y \rangle)^2 - \sum_{i=1}^{N}[y_i - g(x_i)]^2}{\sum_{i=1}^{N}(y_i - \langle y \rangle)^2}$$

where $g(x_i)$ denotes the regression curve and $\langle y \rangle$ the average of the time series $y(t)$ over $N$ samples [note that the same procedure may be carried out by binning $y(t)$ and computing the expected values of $x(t)$]. The nonlinear coefficient can take values between 0 [when $x(t)$ and $y(t)$ are independent] and 1 (in case of a perfect dependency). If the underlying relationship is linear, the $h^2$ approximates the common linear correlation coefficient, $r^2$.

The nonlinear index is able to describe the dependency of the signals under more general types of relationship and produces an asymmetric function, i.e., $h^2 (x \rightarrow y) \neq h^2 (y \rightarrow x)$. This is a very interesting property because the asymmetry can give insight into a possible driving-response relationship. The nonlinear correlation index can be estimated as a function of a time shift ($\tau$), and the shift for which the maximum of $h^2(\tau)$ is reached can be used as an estimate of the time delay between the signals. In the present study, the association between PPN and MCx and their corresponding time delays were obtained by estimating the $h^2$ as a function of a time shift, $\tau(-100 < \tau < 100$ ms), and frequency in the 1- to 100-Hz range (50 frequencies logarithmically distributed) using $L = 10$ bins. Longer shifts (approximately $\pm 5$ s) were also computed for low-frequency signals (delta and theta) using a lower sampling rate (100 Hz); no differences to the above shift values were found. To assess the $h^2$ significance, 100 surrogates were computed where one of the two signals was shifted by a random delay in the 0- to 60-s range. Time shifting of one of the signals keeps the statistical properties of the original time series but breaks the time structure of the interaction, allowing to determine whether the variability of the interaction occurred by chance.

*Statistics.* Estimates of the power spectral density, coherence, and $h^2$ were computed for each recording sample (control, $n = 31$; 6-OHDA, $n = 28$). Data are expressed as means and SE. Cluster-based, nonparametric permutation $t$-tests ($n = 1,000$ permutations) were used to account for the lesion effects on the spectral content of the ECoG and PPN signals (Fig. 1, *A* and *B*), coherence estimates (Fig. 1*C*), and $h^2$ (Fig. 2*A*) across all frequency bands (Maris and Oostenveld 2007). Lesion effects in the strength (Fig. 2, *B* and *C*) and delays (Fig. 3*C*) of the cortico-PPN interaction for each frequency band were assessed using the Mann-Whitney $U$ test for equal medians,

and test for zero-lag interactions was carried out by computing a nonparametric test (sign test) against the null hypothesis of zero median (Fig. 3*B*).

## RESULTS

We recorded ECoG activity from the MCx and the LFPs from the PPN of urethane- and ketamine/xylazine-anesthetized rats during periods of cortical activation (i.e., absence of slow oscillations). Cortical activation episodes occurred either spontaneously (Clement et al. 2008) or following sensory stimulation. Welch periodogram analysis showed that the predominant activity in the cortex of control rats was in the delta (1–4 Hz) and gamma (30–70 Hz) ranges (Fig. 1*A*). 6-OHDA-lesioned rats also showed activity in the delta and gamma ranges but more prominently in the beta (12–30 Hz) range, as has been reported previously in basal ganglia structures (Brazhnik et al. 2012; Mallet et al. 2008; Sharott et al. 2005). Statistical differences were observed in the 15- to 36-Hz range ($P = 0.014$). Recordings from the PPN in both control and 6-OHDA rats showed significantly different activity in the delta-theta-low-alpha range (4–10 Hz; $P = 0.039$; maximum peak = 4 Hz), but no evident peak in the beta range was observed (Fig. 1*B*). For higher frequencies, the spectra of both signals decay monotonically, and no prominent activity was detected in any condition.

To test for linear interactions between MCx and PPN, we estimated the coherence as has been widely used for studying interactions between different brain structures. It can be used to assess the existence of functional interactions, ranging from 0, when there is no association between two signals, to 1, when there is a perfectly linear association between them. We detected two prominent bands of coherent activity between the MCx and PPN in the delta-theta and beta-gamma ranges (Fig. 1*C*). In 6-OHDA rats, these same bands of coherent activity were identified, but an additional prominent band in the alpha-low-beta range (10–14 Hz) that was statistically different ($P = 0.021$) from control rats was also detected.

Once we identified significant coherent activity between MCx and PPN, we then examined their causal interactions. For
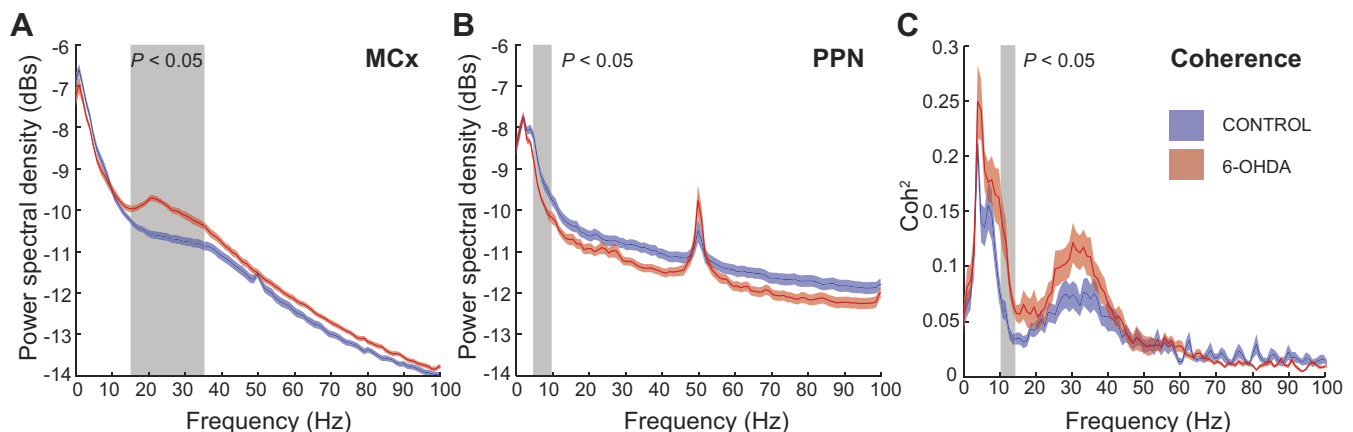


Fig. 1. Coherent activity between the motor cortex (MCx) and the pedunculopontine nucleus (PPN) is observed across different frequency ranges. *A* and *B*: power spectral density (PSD) of the cortical (*A*) and PPN (*B*) oscillatory activity shows an increase in the power of beta and gamma frequency bands in the MCx of rats that received a 6-hydroxydopamine (6-OHDA) lesion, which were not evident in the PPN. In turn, significant differences were observed in the theta-alpha bands in the PPN between conditions. *C*: the local field potentials of the MCx and PPN show 2 wide bands of coherent activity (measured by the squared coherence, Coh²) comprising the theta-alpha ranges and the beta-gamma ranges. These were significantly different between experimental conditions around 10 Hz. Data are depicted as means ± SE, blue traces for control animals, red for 6-OHDA. Shaded area depicts spectral regions where significant differences in power or coherence between control and 6-OHDA conditions were detected (see text).
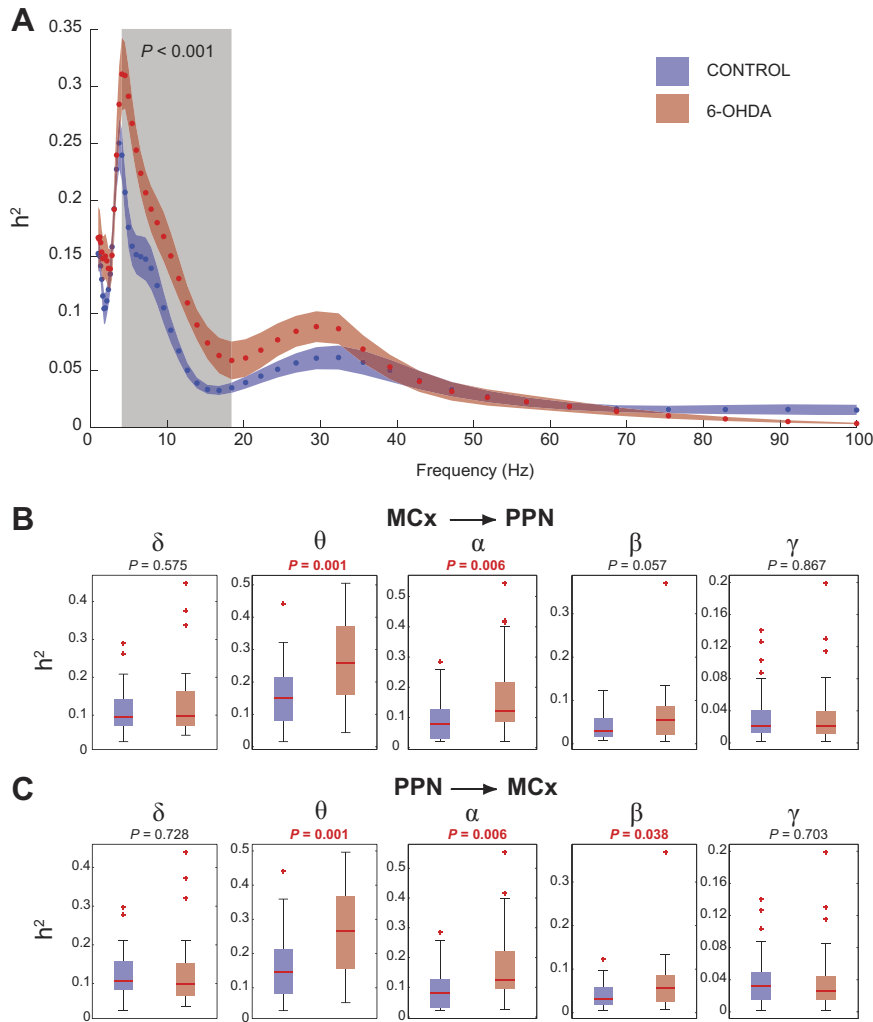
Fig. 2. Increased cortical drive of PPN oscillatory activity is predominantly observed in the alpha range. *A*: the comparison of the nonlinear correlation coefficient ($h^2$) between groups shows significant differences in the 4- to 18-Hz range (shaded box; see text). Data are depicted as means ± SE, blue for control animals, red for 6-OHDA. *B* and *C*: the computation of the $h^2$ for each band (delta, 1–4 Hz; theta, 4–7 Hz; alpha, 8–12 Hz; beta, 12–30 Hz; and gamma, 30–70 Hz) detected significant differences in the theta and alpha ranges when $h^2$ was referenced to the MCx (*B*) and in the theta, alpha, and beta ranges when $h^2$ was referenced to the PPN (*C*). Data in *B* and *C* are depicted as medians (red lines) and 90 and 95% confidence intervals; red crosses represent outliers.

this, we used the $h^2$. Unlike coherence, this parameter allows the detection of both linear and nonlinear associations between two signals with the added possibility of determining the delay between them. We observed similar results as with the coherence analysis when the $h^2$ was obtained (Fig. 2*A*), thus suggesting that the nature of the detected interaction is mainly linear. Significant differences between control and lesioned animals were observed in the range of 4.9–16.7 Hz ($P = 0.001$) using a cluster-based nonparametric permutation test on the full spectral range. Similar to the coherence analysis (Fig. 1*C*), the $h^2$ analysis also detected a band of interaction in the beta-gamma range, although such differences were not significant. Analysis of the $h^2$ interactions within each of the classical bands (Fig. 2, *B* and *C*) revealed results consistent with the full spectral analysis. We detected highly significant differences between control and 6-OHDA rats in the theta (4–7 Hz) and alpha (8–12 Hz) bands (see figures for *P* values). Moreover, and due to the asymmetry of the $h^2$ estimator, we also detected significant differences in the beta band (12–30 Hz) when the signal from PPN was considered as the driver (Fig. 2*C*).

As stated above, the asymmetry of the $h^2$ also allowed the quantification of the delay for the interactions across the different frequencies (Fig. 3*A*). This is an important point as the existence of lagged interactions rules out the possibility of

spurious effects due to volume conduction and allows to ascribe causality to the signals, i.e., identify which one leads the other. We calculated the delay in the interaction between MCx and PPN in those cases with significant $h^2$ values (Fig. 3*B*). When considering the MCx as driver, we observed that at most frequency bands the majority of cases showed a delay significantly greater than zero (Fig. 3*B*), thus suggesting a predominantly unidirectional interaction. The analysis of these delays detected the presence of nonzero delay interactions for theta and gamma in both control and 6-OHDA rats and only for beta in controls and alpha in 6-OHDA rats, suggesting meaningful interactions between MCx and PPN in these frequency ranges that are not the product of volume conduction. Interestingly, the presence of zero-lag interactions in the beta range of 6-OHDA rats, given the prominent activity observed in the cortex, suggests the involvement of third-party structures interacting with the PPN (see DISCUSSION). We then compared the time delays between control and 6-OHDA rats in all frequency ranges (Fig. 3*C*) and detected a significant difference only in the gamma range, where the delay is significantly lower in parkinsonian rats (5.5 ms in controls and 4 ms in 6-OHDA rats). The consistency of this interaction in the gamma band in most of the cases evaluated in both conditions (Fig. 3*B*), taken together with the results from the coherence and $h^2$ analyses in the alpha band, suggest a robust direct commu-
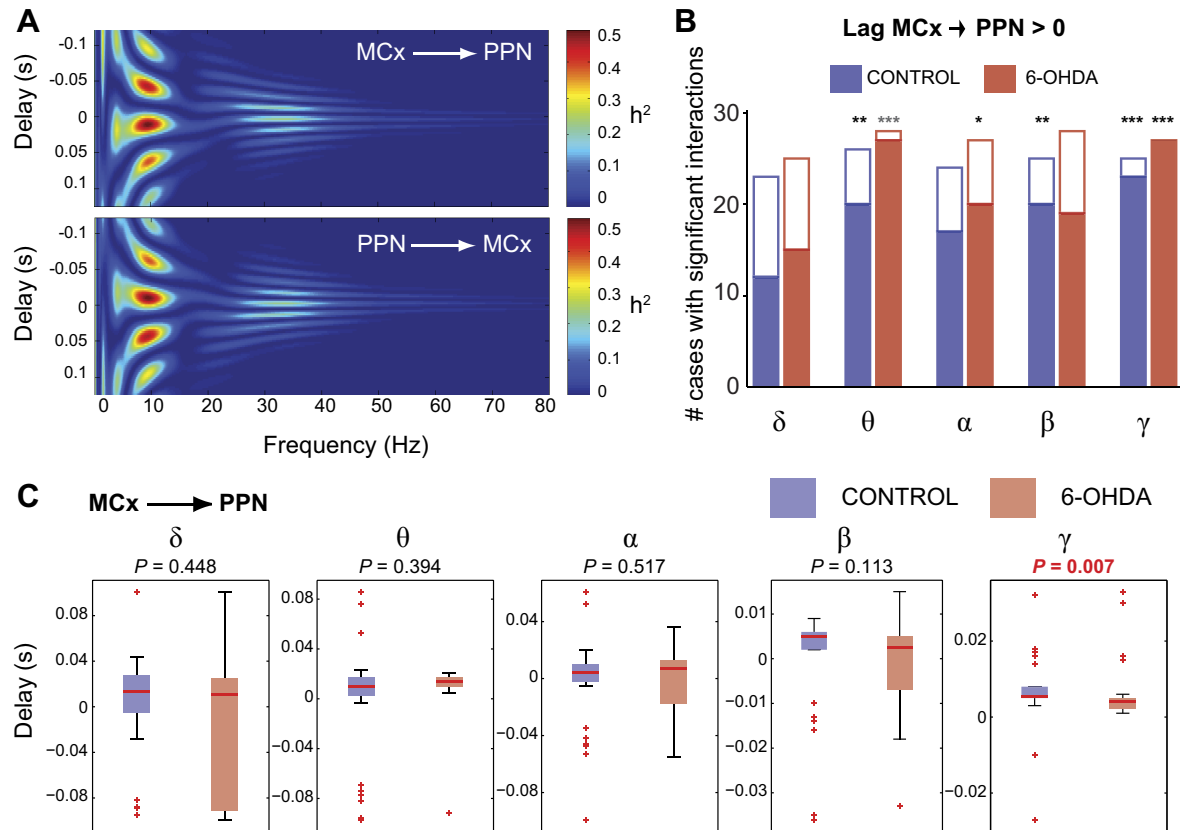
Fig. 3. Consequences of dopamine depletion on the delay of interaction between MCx and PPN. *A*: the nonlinear correlation coefficient $h^2$ was used to determine the delays across the whole set of spectral frequencies. *B*: the majority of cases showed a delay that was significantly different from 0 for all frequencies but delta, suggesting a wide-band cortical drive (empty bars indicate negative delays, filled bars indicate positive delays; *$P < 0.05$, **$P < 0.01$, ***$P < 0.001$; i.e., the lower the *P* value, the larger the proportion of significant interactions within each band). #, Number of. *C*: differences in the delay of interaction between MCx and PPN were only detected for the gamma band that showed significantly shorter delays in the lesioned rats. Data are depicted as medians (red lines) and 90 and 95% confidence intervals; red crosses represent outliers.

nication between both structures that is accentuated in the parkinsonian condition.

## DISCUSSION

Recently, several efforts have been made to understand the pathophysiology of the PPN in PD and its contribution to the motor disturbances of the disease (Benarroch 2013). The PPN is a complex heterogeneous structure for which functions are associated with the generation of oscillatory activity in its targets (Mena-Segovia and Bolam 2011). Here, we aimed to understand the involvement of the PPN in fast frequency oscillations ($>1$ Hz) in normal animals and following lesions of the nigrostriatal pathway. We observed an increase in the oscillatory activity in the cortex of parkinsonian rats in the beta-gamma range, as has been reported previously (Brazhnik et al. 2012; Sharott et al. 2005). Although this frequency range was barely present in the PPN of lesioned rats, it did show a coherent activity with the cortex, but this was not significantly different between control and lesioned rats. In contrast, we observed significant coherent activity between the MCx and PPN in the alpha range, and this was significantly larger in parkinsonian rats, supporting the theory of hypersynchronization in corticobasal ganglia-thalamocortical circuits (Dejean et al. 2008; Hammond et al. 2007; Quiroga-Varela et al. 2013).

Estimations of the nonlinear interactions between MCx and PPN revealed increased $h^2$ values in the theta and alpha bands

in lesioned rats, suggesting stronger functional connectivity following dopaminergic denervation. These findings are in line with previous reports showing increased coherent activity between cortex and PPN of 6-OHDA-lesioned rats during slow-wave activity (Aravamuthan et al. 2008) and between cortex and other basal ganglia nuclei (Brazhnik et al. 2012; Sharott et al. 2005). It may be possible to interpret these findings in the context of an increased reactivity of PPN neurons, as suggested by the decreased habituation to sensory stimulation in PD patients (Teo et al. 1997). However, subclasses of PPN neurons may respond differently to distinct driving frequency oscillations. On the other hand, we only observed a small effect in the beta band that was not bidirectional (only significantly different when the PPN was used as the reference). This is an interesting observation given the prominent activity of the cortex in this band, which seems not to be directly related to the PPN activity but perhaps with other intermediate structures (e.g., STN; Aravamuthan et al. 2007; Florio et al. 2007; Hammond et al. 1983). One possible explanation considers the dynamic nature of this abnormal beta activity, suggested at least in part by the high heterogeneity within this band in lesioned rats (Fig. 3*B*), but this would require different approaches and further analysis.

We then calculated the delay in the interaction between cortex and PPN across different frequency bands. In the vast majority of cases, we observed that the cortex was leading the

PPN, with positive delays significantly different from zero. This suggests that, more often than not, during the activated-like state of the urethane-anesthetized rat, the cortex drives PPN irrespective of the frequency band. In a minority of cases, it was not possible to determine the delay because of volume conduction (i.e., 0 delay). When such delays were compared between conditions, we observed that only gamma was significantly different. Thus 6-OHDA-lesioned rats showed a shorter delay in the interaction between MCx and PPN, further supporting the idea of abnormal connectivity in parkinsonian rats.

In summary, we detected an increased interaction in the alpha band between the MCx and the PPN of 6-OHDA-lesioned rats and a faster interaction in the gamma band, in line with similar findings in other basal ganglia structures (Dejean et al. 2008). Recent reports have shown the presence of a peak in the alpha band in the PPN of PD patients (recorded from the DBS electrode) that is coherent with cortical activity (Androulidakis et al. 2008; Thevathasan et al. 2012b). Our findings in the 6-OHDA rat reflect the findings in PD patients and show that such coherent activity is different between dopamine-intact and dopamine-depleted animals. This suggests a basic mechanism of communication between the MCx and the PPN that is altered in the parkinsonian condition. In agreement with our findings in 6-OHDA rats, PD patients show a decreased alpha power compared with recordings following L-DOPA administration (Androulidakis et al. 2008), but, in contrast to our results, L-DOPA treatment seems to increase the coherence between PPN and cortex. In addition, it was observed in the same study that the interaction between structures was bidirectional. These differences between patients and the model are possibly related to the brain state and behavioral context (awake and performing in humans vs. anesthesia in rats), suggesting that the drive from the PPN in the anesthetized rat is diminished, thus increasing the cortical drive and consequently the coherence. Furthermore, we also observed a reduced delay between gamma band signals recorded from the MCx and the PPN. Because gamma oscillations have been suggested to provide the temporal structure to bind and facilitate neuronal communications (Nikolic et al. 2013) and since some neurons in the PPN can potentially fire at gamma frequencies (Kezunovic et al. 2011), the enhanced (faster) interaction with the cortex could potentially have an impact on the PPN neuronal activity. Depending on the neuronal subtypes involved, this will therefore produce different effects on PPN targets (Martinez-Gonzalez et al. 2013).

*Conclusions.* We report that the MCx and the PPN interact across two frequency bands: alpha and gamma. Although these interactions are present in both control and 6-OHDA-lesioned rats, we observe a significantly increased interaction in the alpha band of parkinsonian rats. In contrast, in the gamma band, although the correlation between MCx and PPN is similar, the delay between these signals is shorter in parkinsonian rats. In most of the cases, MCx was leading the PPN, which may be a consequence of the anesthesia. Our results suggest a robust channel of communication through which cortex interacts with the brain stem and that is susceptible to dysfunction following the chronic dopamine depletion.

## REFERENCES

**Androulidakis AG, Mazzone P, Litvak V, Penny W, Dileone M, Gaynor LM, Tisch S, Di Lazzaro V, Brown P.** Oscillatory activity in the pedunculopontine area of patients with Parkinson's disease. *Exp Neurol* 211: 59–66, 2008.

**Aravamuthan BR, Bergstrom DA, French RA, Taylor JJ, Parr-Brownlie LC, Walters JR.** Altered neuronal activity relationships between the pedunculopontine nucleus and motor cortex in a rodent model of Parkinson's disease. *Exp Neurol* 213: 268–280, 2008.

**Aravamuthan BR, Muthusamy KA, Stein JF, Aziz TZ, Johansen-Berg H.** Topography of cortical and subcortical connections of the human pedunculopontine and subthalamic nuclei. *Neuroimage* 37: 694–705, 2007.

**Avila I, Parr-Brownlie LC, Brazhnik E, Castaneda E, Bergstrom DA, Walters JR.** Beta frequency synchronization in basal ganglia output during rest and walk in a hemiparkinsonian rat. *Exp Neurol* 221: 307–319, 2010.

**Benarroch EE.** Pedunculopontine nucleus: functional organization and clinical implications. *Neurology* 80: 1148–1155, 2013.

**Brazhnik E, Cruz AV, Avila I, Wahba MI, Novikov N, Ilieva NM, McCoy AJ, Gerber C, Walters JR.** State-dependent spike and local field synchronization between motor cortex and substantia nigra in hemiparkinsonian rats. *J Neurosci* 32: 7869–7880, 2012.

**Breit S, Bouali-Benazzouz R, Benabid AL, Benazzouz A.** Unilateral lesion of the nigrostriatal pathway induces an increase of neuronal activity of the pedunculopontine nucleus, which is reversed by the lesion of the subthalamic nucleus in the rat. *Eur J Neurosci* 14: 1833–1842, 2001.

**Brown P.** Bad oscillations in Parkinson's disease. *J Neural Transm Suppl* 27–30, 2006.

**Caliandro P, Insola A, Scarnati E, Padua L, Russo G, Granieri E, Mazzone P.** Effects of unilateral pedunculopontine stimulation on electromyographic activation patterns during gait in individual patients with Parkinson's disease. *J Neural Transm* 118: 1477–1486, 2011.

**Clement EA, Richard A, Thwaites M, Ailon J, Peters S, Dickson CT.** Cyclic and sleep-like spontaneous alternations of brain state under urethane anaesthesia. *PLoS One* 3: e2004, 2008.

**Dejean C, Gross CE, Bioulac B, Boraud T.** Dynamic changes in the cortex-basal ganglia network after dopamine depletion in the rat. *J Neurophysiol* 100: 385–396, 2008.

**Dejean C, Nadjar A, Le Moine C, Bioulac B, Gross CE, Boraud T.** Evolution of the dynamic properties of the cortex-basal ganglia network after dopaminergic depletion in rats. *Neurobiol Dis* 46: 402–413, 2012.

**Donoghue JP, Wise SP.** The motor cortex of the rat: cytoarchitecture and microstimulation mapping. *J Comp Neurol* 212: 76–88, 1982.

**Florio T, Scarnati E, Confalone G, Minchella D, Galati S, Stanzione P, Stefani A, Mazzone P.** High-frequency stimulation of the subthalamic nucleus modulates the activity of pedunculopontine neurons through direct activation of excitatory fibres as well as through indirect activation of inhibitory pallidal fibres in the rat. *Eur J Neurosci* 25: 1174–1186, 2007.

**Halliday DM, Rosenberg JR, Amjad AM, Breeze P, Conway BA, Farmer SF.** A framework for the analysis of mixed time series/point process data–theory and application to the study of physiological tremor, single

motor unit discharges and electromyograms. *Prog Biophys Mol Biol* 64: 237–278, 1995.

**Hammond C, Bergman H, Brown P.** Pathological synchronization in Parkinson's disease: networks, models and treatments. *Trends Neurosci* 30: 357–364, 2007.

**Hammond C, Rouzaire-Dubois B, Feger J, Jackson A, Crossman AR.** Anatomical and electrophysiological studies on the reciprocal projections between the subthalamic nucleus and nucleus tegmenti pedunculopontinus in the rat. *Neuroscience* 9: 41–52, 1983.

**Healy-Stoffel M, Ahmad SO, Stanford JA, Levant B.** Altered nucleolar morphology in substantia nigra dopamine neurons following 6-hydroxydopamine lesion in rats. *Neurosci Lett* 546: 26–30, 2013.

**Heise CE, Teo ZC, Wallace BA, Ashkan K, Benabid AL, Mitrofanis J.** Cell survival patterns in the pedunculopontine tegmental nucleus of methyl-4-phenyl-1,2,3,6-tetrahydropyridine-treated monkeys and 6OHDA-lesioned rats: evidence for differences to idiopathic Parkinson disease patients? *Anat Embryol (Berl)* 210: 287–302, 2005.

**Hirsch EC, Graybiel AM, Duyckaerts C, Javoy-Agid F.** Neuronal loss in the pedunculopontine tegmental nucleus in Parkinson disease and in progressive supranuclear palsy. *Proc Natl Acad Sci USA* 84: 5976–5980, 1987.

**Kezunovic N, Urbano FJ, Simon C, Hyde J, Smith K, Garcia-Rill E.** Mechanism behind gamma band activity in the pedunculopontine nucleus. *Eur J Neurosci* 34: 404–415, 2011.

**Kringelbach ML, Jenkinson N, Owen SL, Aziz TZ.** Translational principles of deep brain stimulation. *Nat Rev Neurosci* 8: 623–635, 2007.

**Leszkowicz E, Kusmierczak M, Matulewicz P, Trojniar W.** Modulation of hippocampal theta rhythm by the opioid system of the pedunculopontine tegmental nucleus. *Acta Neurobiol Exp (Warsz)* 67: 447–460, 2007.

**Lopes da Silva F, Pijn JP, Boeijinga P.** Interdependence of EEG signals: linear vs. nonlinear associations and the significance of time delays and phase shifts. *Brain Topogr* 2: 9–18, 1989.

**Lopez-Azcarate J, Tainta M, Rodriguez-Oroz MC, Valencia M, Gonzalez R, Guridi J, Iriarte J, Obeso JA, Artieda J, Alegre M.** Coupling between beta and high-frequency activity in the human subthalamic nucleus may be a pathophysiological mechanism in Parkinson's disease. *J Neurosci* 30: 6667–6677, 2010.

**Lorincz ML, Crunelli V, Hughes SW.** Cellular dynamics of cholinergically induced alpha (8–13 Hz) rhythms in sensory thalamic nuclei in vitro. *J Neurosci* 28: 660–671, 2008.

**Magill PJ, Bolam JP, Bevan MD.** Dopamine regulates the impact of the cerebral cortex on the subthalamic nucleus-globus pallidus network. *Neuroscience* 106: 313–330, 2001.

**Mallet N, Pogosyan A, Marton LF, Bolam JP, Brown P, Magill PJ.** Parkinsonian beta oscillations in the external globus pallidus and their relationship with subthalamic nucleus activity. *J Neurosci* 28: 14245–14258, 2008.

**Maris E, Oostenveld R.** Nonparametric statistical testing of EEG- and MEG-data. *J Neurosci Methods* 164: 177–190, 2007.

**Martinez-Gonzalez C, Bolam JP, Mena-Segovia J.** Topographical organization of the pedunculopontine nucleus. *Front Neuroanat* 5: 22, 2011.

**Martinez-Gonzalez C, van Andel J, Bolam JP, Mena-Segovia J.** Divergent motor projections from the pedunculopontine nucleus are differentially regulated in Parkinsonism. *Brain Struct Funct*. First published May 26, 2013; doi:10.1007/s00429-013-0579-6.

**Mena-Segovia J, Bolam JP.** Phasic modulation of cortical high-frequency oscillations by pedunculopontine neurons. *Prog Brain Res* 193: 85–92, 2011.

**Mena-Segovia J, Bolam JP, Magill PJ.** Pedunculopontine nucleus and basal ganglia: distant relatives or part of the same family? *Trends Neurosci* 27: 585–588, 2004.

**Mena-Segovia J, Micklem BR, Nair-Roberts RG, Ungless MA, Bolam JP.** GABAergic neuron distribution in the pedunculopontine nucleus defines functional subterritories. *J Comp Neurol* 515: 397–408, 2009.

**Mena-Segovia J, Sims HM, Magill PJ, Bolam JP.** Cholinergic brainstem neurons modulate cortical gamma activity during slow oscillations. *J Physiol* 586: 2947–2960, 2008.

**Moro E, Hamani C, Poon YY, Al-Khairallah T, Dostrovsky JO, Hutchison WD, Lozano AM.** Unilateral pedunculopontine stimulation improves falls in Parkinson's disease. *Brain* 133: 215–224, 2010.

**Nikolic D, Fries P, Singer W.** Gamma oscillations: precise temporal coordination without a metronome. *Trends Cogn Sci* 17: 54–55, 2013.

**Pahapill PA, Lozano AM.** The pedunculopontine nucleus and Parkinson's disease. *Brain* 123: 1767–1783, 2000.

**Paxinos G, Watson C.** *The Rat Brain in Stereotaxic Coordinates*. San Diego, CA: Academic Press, 1986, p. 119.

**Pinault D.** A novel single-cell staining procedure performed in vivo under electrophysiological control: morpho-functional features of juxtacellularly labeled thalamic cells and other central neurons with biocytin or Neurobiotin. *J Neurosci Methods* 65: 113–136, 1996.

**Quiroga-Varela A, Walters JR, Brazhnik E, Marin C, Obeso JA.** What basal ganglia changes underlie the parkinsonian state? The significance of neuronal oscillatory activity. *Neurobiol Dis* 58: 242–248, 2013.

**Ros H, Magill PJ, Moss J, Bolam JP, Mena-Segovia J.** Distinct types of non-cholinergic pedunculopontine neurons are differentially modulated during global brain states. *Neuroscience* 170: 78–91, 2010.

**Sharott A, Magill PJ, Harnack D, Kupsch A, Meissner W, Brown P.** Dopamine depletion increases the power and coherence of beta-oscillations in the cerebral cortex and subthalamic nucleus of the awake rat. *Eur J Neurosci* 21: 1413–1422, 2005.

**Steriade M.** Corticothalamic resonance, states of vigilance and mentation. *Neuroscience* 101: 243–276, 2000.

**Steriade M, Dossi RC, Pare D, Oakson G.** Fast oscillations (20–40 Hz) in thalamocortical systems and their potentiation by mesopontine cholinergic nuclei in the cat. *Proc Natl Acad Sci USA* 88: 4396–4400, 1991.

**Teo C, Rasco L, al-Mefty K, Skinner RD, Boop FA, Garcia-Rill E.** Decreased habituation of midlatency auditory evoked responses in Parkinson's disease. *Mov Disord* 12: 655–664, 1997.

**Thevathasan W, Cole MH, Graepel CL, Hyam JA, Jenkinson N, Brittain JS, Coyne TJ, Silburn PA, Aziz TZ, Kerr G, Brown P.** A spatiotemporal analysis of gait freezing and the impact of pedunculopontine nucleus stimulation. *Brain* 135: 1446–1454, 2012a.

**Thevathasan W, Pogosyan A, Hyam JA, Jenkinson N, Foltynie T, Limousin P, Bogdanovic M, Zrinzo L, Green AL, Aziz TZ, Brown P.** Alpha oscillations in the pedunculopontine nucleus correlate with gait performance in parkinsonism. *Brain* 135: 148–160, 2012b.

**Trottenberg T, Fogelson N, Kuhn AA, Kivi A, Kupsch A, Schneider GH, Brown P.** Subthalamic gamma activity in patients with Parkinson's disease. *Exp Neurol* 200: 56–65, 2006.

**Wang HL, Morales M.** Pedunculopontine and laterodorsal tegmental nuclei contain distinct populations of cholinergic, glutamatergic and GABAergic neurons in the rat. *Eur J Neurosci* 29: 340–358, 2009.